Influence of the interface structure on the thermo-mechanical properties of Cu-X (X = Cr or B)/carbon fiber composites

Amélie Veillere, Jean-Marc Heintz, Namas Chandra, Joël Douin, Michel Lahaye, Grégory Lalet, Cécile Vincent, Jean-François Silvain

Influence of the interface structure on the thermo-mechanical properties of Cu–X (X = Cr or B)/carbon fiber composites

A. Veillère [a,*], J.-M. Heintz [a], N. Chandra [b], J. Douin [c], M. Lahaye [a], G. Lalet [a], C. Vincent [a], J.-F. Silvain [a]

[a] CNRS, Université de Bordeaux, ICMCB, 87 Avenue du Docteur Albert Schweitzer, 33608 Pessac, France
[b] Engineering Mechanics, University of Nebraska-Lincoln, Lincoln, NE 68588-0642, USA
[c] CNRS, CEMES, 29 Rue Jeanne Marvig, F-31055 Toulouse, France

A B S T R A C T

This study focuses on the fabrication, for power electronics applications, of adaptive heat sink material using copper alloys/carbon fibers (CF) composites. In order to obtain composite material with good thermal conductivity and a coefficient of thermal expansion close to the ceramic substrate, it is necessary to have a strong matrix/reinforcement bond. Since there is no reaction between copper and carbon, a carbide element (chromium or boron) is added to the copper matrix to create a strong chemical bond. Composite materials (Cu–B/CF and Cu–Cr/CF) have been produced by a powder metallurgy process followed by an annealing treatment in order to create the carbide at the interphase. Chemical (Electron Probe Micro-Analysis, Auger Electron Spectroscopy) and microstructural (Scanning and Transmission Electron Microscopies) techniques were used to study the location of the alloying element and the carbide formation before and after diffusion. Finally, the thermo-mechanical properties have been measured and a promising composite material with a coefficient of thermal expansion 25% lower than a classic copper/carbon heat sink has been obtained.

1. Introduction

In the field of power electronics, the size of the electronic devices is continually decreasing as their number are increasing, resulting in higher power and heat dissipated by the package. In the past 40–50 years, different types of metal matrix composites (MMCs), especially with aluminum and copper matrices, have been investigated to try to solve this problem of thermal management of Silicon chips [1–3]. It is necessary to dissipate the excess thermal energy in order to prevent heating and consequent deterioration of the Silicon chip. The material system of choice should not only have a very good thermal dissipation, but high reliability. The latter is greatly limited by the critical difference between the coefficients of thermal expansion (CTE) of the heat sink (generally in copper, $17 \times 10_{6}^{-6}$ K^{-1}), and of the ceramic substrate (mainly alumina, 8×10^{-6} K^{-1}) [4]. More recently, MMCs made with copper reinforced by diamond particles have been investigated to replace the bulk copper heat sink [5–7]. These kinds of MMCs improve the thermo-mechanical properties compared to those of copper, but to achieve these results 60 vol.% of diamond was added in the matrix, and such amount implies a very difficult machinability of the composite for industrial applications.

* Corresponding author. Tel.: +33 5 40 00 62 57; fax: +33 5 40 00 83 21.
E-mail address: veillere@icmcb-bordeaux.cnrs.fr (A. Veille`re).

Alternatively, the use of CF as reinforcement in copper matrices offer a good compromise between thermo-mechanical properties and high conductivity, as well as offering a lower density than copper and good machinability. In a composite, general mechanical and/or physical properties are linked to the properties of the matrix, the reinforcement and the interfacial zone. The major problem in the development of the Cu/CF composites is the absence of chemical reaction between copper and carbon. Indeed, after several thermal cyclings the initial mechanical bonding (induced by the CTE mismatch between copper and carbon, after cooling) is degraded, thus leading to a weak interface and a bad transfer of properties between the matrix and the reinforcement [5–9]. To solve this problem, an alloying element such as chromium or boron is added to the copper matrix in order to confer, after diffusion, a strong chemical interface. This paper presents a detailed characterization of such interfaces, in terms of chemical and microstructural analyses, and establishes a link between these interfacial properties and the thermo-mechanical properties of the MMCs.

2. Experimental methods

2.1. Materials

Chromium and boron have been selected as additive elements to the copper matrix because they react with carbon to form

Table 1
Parameters and thermal properties of the investigated CF.

Fibers	Diameter (μm)	Length (μm)	Density ($g\,cm^{-3}$)	Thermal conductivity ($W\,m^{-1}\,K^{-1}$)		CTE ($10^{-6}\,K^{-1}$)	
				Axial	Transverse	Axial	Transverse
CN80C	10	100–400	2.1	320	5	−1.0	12
XN100	10	100–400	2.1	900	5	−1.0	12

carbide compounds (negative Gibbs energy) [10]. The copper-based alloys are Cu–B (0.05 wt.% of B) and Cu–Cr (0.63 wt.% of Cr). The amounts of boron and chromium have been chosen in order to have the alloying element in solid solution in copper and prevent the formation of particles inside the matrix, which can decrease the thermal properties. The powders are prepared by CERAM (United Kingdom), by an atomization process, with a particle size under 25 μm. Two kinds of chopped CF, manufactured by Nippon Graphite Fiber Corporation, are investigated. Both have a diameter of 10 μm, a length ranging from 100 to 400 μm, and a CTE of $-1.0 \times 10^{-6}\,K^{-1}$ and $12 \times 10^{-6}\,K^{-1}$ along and perpendicular to their axis, respectively. The difference between these two kinds of CF is their thermal conductivity along their axis which is about 320 $W\,m^{-1}\,K^{-1}$ and 900 $W\,m^{-1}\,K^{-1}$ for the CN80C and XN100, respectively (Table 1). It has to be mentioned that the thermal conductivity measured perpendicular to the fiber axis is equivalent for both fiber and in the order of 5 $W\,m^{-1}\,K^{-1}$.

Copper alloy powders are mechanically mixed with CF (volume fraction equal to 30%) and are then uniaxially hot pressed at 950 °C under 50 MPa for 20 min to obtain dense materials. During the sintering cycle, a reducing atmosphere of argon/hydrogen (5 vol.%) is used to first deoxidize the initial Cu alloys powder and then prevent the oxidation of the copper during densification. An optimized annealing treatment is then performed (1000 °C, 24 h, under reducing atmosphere) on the most promising composite (Cu–Cr/CN80C) to increase the diffusion of the alloying element (Cr) toward the Cu/CF interface and therefore create stronger carbide interface bonds.

2.2. Chemical and microstructural characterizations

After densification, the samples were analyzed in cross and parallel section using an optical microscope (Olympus PMG3). Matrix, interface and reinforcement microstructures were analyzed using scanning electron microscopy (SEM, JEOL 6700F). In order to investigate the microstructure of the interface at a nanometric scale, transmission electron microscopy was also used (TEM, JEOL 200CX).

The chemical distribution of the alloying element inside the composite was analyzed using Electron Probe Micro-Analyses (EPMA, CAMECA SX 100) equipped with wavelength dispersive spectrometry (WDS); the accelerating voltage was 20 kV. Auger Electron Spectroscopy (AES, VG Microlab 310F) was used in order to analyze the chemical composition of the matrix, reinforcement and interfaces at a nanometric scale (analyses diameter around 30 nm). The AES analyses were made with an acceleration voltage of 10 keV and a beam current of 4 nA. The energy ranges investigated in this technique were the following for each element: 890–950 eV (Cu_{LM2}), 520–600 eV (Cr_{LM2}) and 250–275 eV (C_{KL1}). The peaks in the energy spectrum were correlated to an AES database [11] or peaks from reference compounds obtained from the same equipment to identify specific elements. Data acquired along the line profile were computer-analyzed using a non-linear least square fitting (NLLSF). Finally the atomic concentration of each of the identified elements is plotted as a function of distance from a reference point.

2.3. Thermo-mechanical measurements

The thermo-mechanical properties have been measured on each composite material. The thermal diffusivity (α) was measured using a flash laser technique (Netzsch LFA 457). In this technique, a pulse laser excites the bottom-surface of the sample and the variation of temperature is measured in the opposite face. This measure is performed on 6 mm diameter samples and between 2 and 5 mm thick. The faces must be parallel in order to obtain accurate and reproducible results. Before the experiment, the sample is covered with a thin film of graphite to avoid radiation. The thermal conductivity (λ) of the material is deduced using the relation $\lambda = \alpha \cdot \rho \cdot Cp$, where ρ correspond to the density of the composite measured by the Archimedes method and Cp is the specific heat at constant pressure calculated with a rule of mixture.

The coefficient of thermal expansion (CTE) was measured with a differential dilatometer (Netzsch LFA 457). The heating rate was 2 °C/min and ranged from room temperature to 250 °C under argon atmosphere. The CTE value is an average value measured between 100 °C and 200 °C.

3. Results and discussion

3.1. Densification

The final density of the composite material is close to 97% and no specific degradation of the CF was observed. The optical micrographs of the samples show a strong anisotropic structure (Fig. 1), with an orientation of the CF perpendicular to the pressure direction. This anisotropy is due to the strains and stresses imposed by the pressing conditions and geometry, and will be

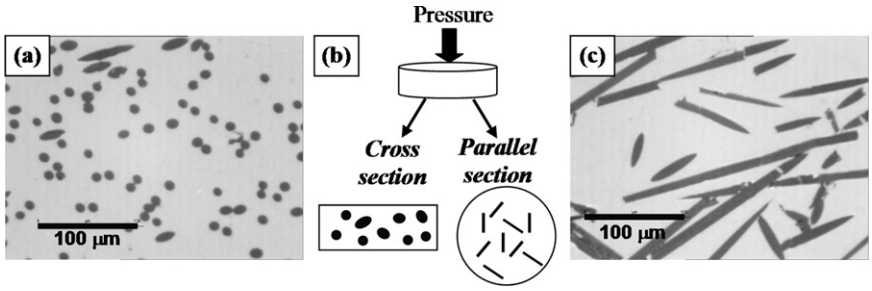

Fig. 1. Optical micrographs of the composite material in (a) cross and (c) parallel section after densification and (b) schematic of the CF orientation.

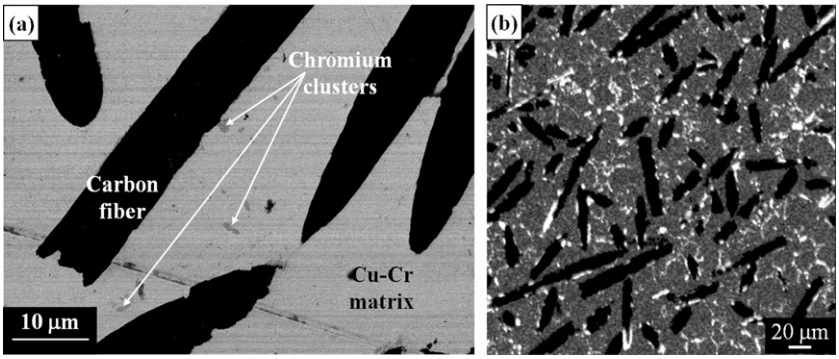

Fig. 2. Back-scattering SEM micrographs of sample S5 (a) before and (b) after annealing treatment at 1000 °C/24 h under Ar/H_2 (5%) atmosphere.

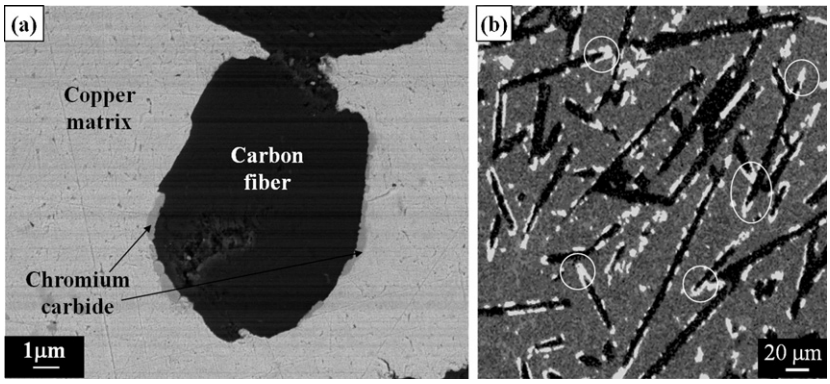

Fig. 3. Chromium EPMA mapping of the initial Cu–Cr powder.

reflected in the anisotropic thermal (λ) and thermo-mechanical (CTE) properties of the composite.

3.2. Microstructure and interface chemistry

Fig. 2a shows a back-scattered SEM micrograph of the Cu–Cr/CF sample before annealing treatment. In this micrograph, the carbon fibers appear in black, the Cu in light gray and the Cr in dark gray. We can observe Cr clusters on the Cu matrix and some at the Cu/CF interfaces. These observations are confirmed by the WDS-EPMA mapping of the Cr in a representative area of the sample (Fig. 2b). The high temperature of the densification process (950 °C) allows partial diffusion of the alloying element toward the interface.

Fig. 3 shows a back-scattered SEM micrograph (Fig. 3a) and the chromium WDS-EPMA mapping (Fig. 3b) of the Cu–Cr/CF sample after an annealing treatment at 1000 °C for 24 h. Both analyses show that most of the Cr has migrated toward the Cu/CF interface and the Cu matrix is almost free of Cr. At this scale of analysis, the alloying element does not appear homogeneously dispersed at the interface, as portions seem without alloying element. The non-uniformity and discontinuity of the interphase could be linked to the inhomogeneous dispersion of the alloying element in the initial copper alloy powders. Fig. 4 shows an EPMA mapping of the Cr in the initial Cu–Cr powder where it is clear that the Cr (in white) is not distributed evenly in the copper grains. This heterogeneity induces a non-uniform diffusion of the alloying element in the copper matrix and may explain the thickness variation of the Cu/CF interfacial zone. We can also observe, circled in Fig. 3b, a higher segregation of Cr on the CF tip. This tip segregation is due to the carbon pending bond present in these areas.

AES line profiles have been obtained across a Cu/CF interphase. One representative line profile is shown in Fig. 5. Atomic concentrations of Cu, C and Cr were measured along the line. A deconvolution of the carbon peak has been applied in order to distinguish the carbon from the chromium carbide (C–Cr bonds) and the free carbon (C–C bonds). This deconvolution process was performed with two reference profiles: one for the free carbon (C–C) and one for the carbon inside the Cr_3C_2 chromium carbide (C–Cr). The figure shows three distinct zones: the matrix, the interphase and the fiber. Both Cr and C–Cr carbon are present only in the interphase. This analysis confirms the segregation of chromium in the form of chromium carbide at the Cu/CF interface. The thickness of the interphase ranges from 0.1 to 1 μm.

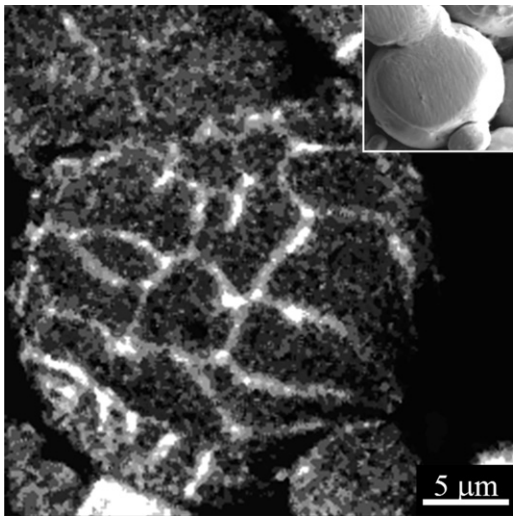

Fig. 4. EPMA mapping of the chromium in sample S5 (a) before and (b) after annealing treatment.

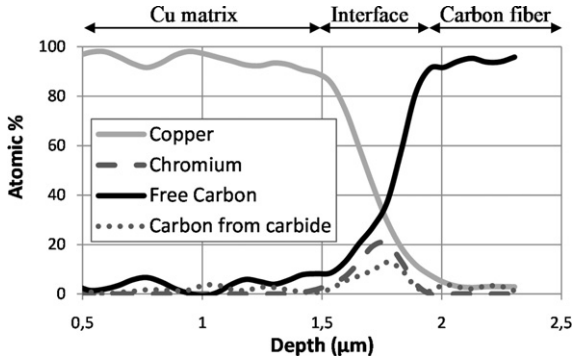

Fig. 5. AES depth profile through the Cu/CF interface of sample S5 after annealing treatment.

Both of these chemical analyses confirm the diffusion, after annealing treatment, of the alloying element through the Cu matrix toward the Cu/CF interface, with the formation of a carbide.

3.3. Interface morphology and crystallographic structure

TEM studies have been performed on both Cu–Cr/CF and Cu–B/CF composite materials, in order to analyze the interface at a nanometric scale and determine its crystallographic structure. The thickness of the carbide interphase has been measured in both cases, ranging from 50 nm to 1 μm. We also notice its presence all around the fiber, contrary to the first SEM observations. Fig. 6 shows TEM micrographs and diffraction patterns obtained on the Cu–B/CF composite. Micrograph 6a shows 3 distinct areas: the matrix, the interfacial zone and the CF, from top to bottom. In this micrograph, the CF is not attached to the interfacial zone, this phenomenon is an artifact due to the thin film preparation for the TEM analyses. The diffraction pattern acquired in the Cu matrix shows the presence of metallic Cu with no trace of alloying element in cluster shape. Therefore if an alloying element was present in the matrix, it would be in a small amount and in a solid solution with Cu. The diffraction pattern of the CF (Fig. 6d) is composed of rings formed by its graphitic plane structure, and of a systematic diffraction line {1 1 1} due to the preferential orientation of the graphitic planes along the fiber axis. A typical diffraction pattern obtained at the interphase area reveals a ring-like morphology which is characteristic of polycrystalline grains with sizes much smaller than the diffraction diaphragm used to obtain that pattern (10 μm). The indexation of the rings clearly shows the presence of boron carbide B_4C ($R\bar{3}m$ space group). A zoom on the interfacial zone is shown in Fig. 6e and a dark field of the same zone using the {1 0 4} B_4C diffraction ring can be seen in Fig. 6f. From these micrographs, we can observe the nanometric size (between 5 and 30 nm) of B_4C grains (in white). The same analyses have been performed on the Cu–Cr/CF composite material (Fig. 7a–c). Three zones are visible (Fig. 7a and b) and the electronic diffraction analyses (Fig. 7c) of each zone identified the crystallographic structures of the Cu matrix, the CF and the interfacial zone composed of chromium carbide Cr_3C_2 (*Pnma* space group).

3.4. Thermo-mechanical properties

The thermal conductivity (TC) and the coefficient of thermal expansion (CTE) of each material have been measured. Both TC and CTE depend on the quality of the matrix/reinforcement interface [13]. Two kinds of interfaces can be defined:

- A mechanical interface due to the mechanical clamping arising from CTE mismatch-induced thermal stresses during cooling.

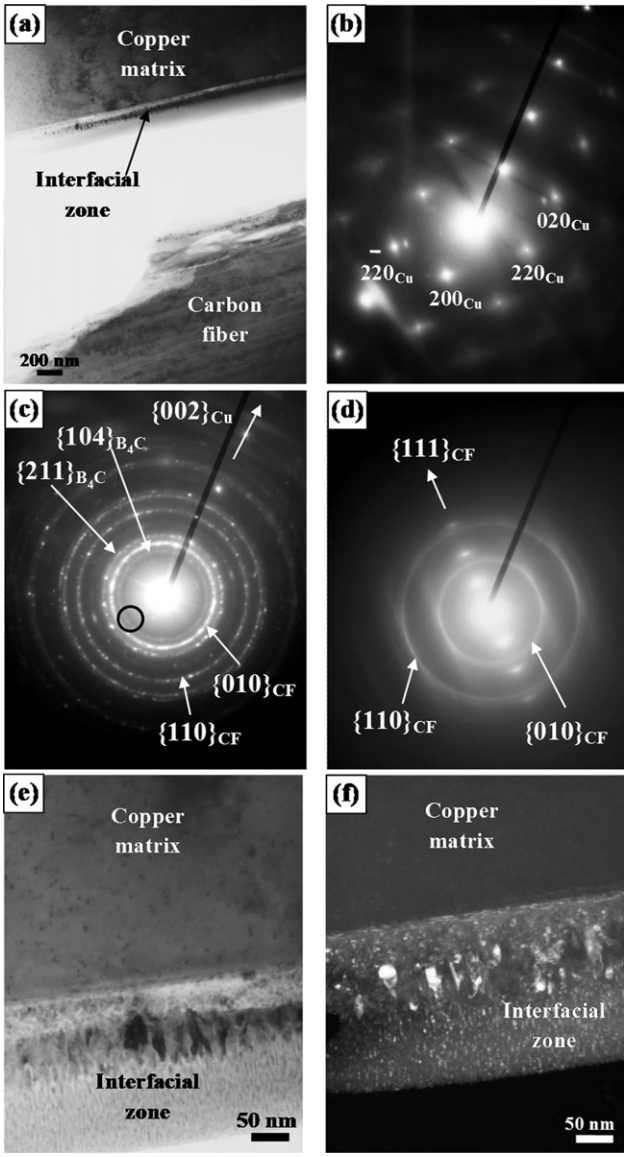

Fig. 6. TEM analyses of sample S9. (a) Bright field of the zone with, from top to bottom, the Cu matrix, the interface and the CF; (b) diffraction pattern of the Cu matrix ([0 0 1] copper axis); (c) diffraction pattern of the interfacial zone; (d) diffraction pattern of the CF; (e) zoom on the interfacial zone and (f) dark field of the interfacial zone using the {1 0 4}B_4C diffraction ring marked on (c).

- A chemical interface due to the formation of carbide (Cr_3C_2 or B_4C) created by the diffusion of the alloying element (Cr or B) at the Cu/CF interface.

In this section, the measured TC and CTE will be related to the matrix, reinforcement and interface type.

3.4.1. Thermal conductivity (TC)

Thermal diffusivity is measured along the pressure direction of the densification process due to technical limitation during the experiments. As shown in Section 3.1, the densification process induces an anisotropic structure in the samples with a preferential orientation of the CF perpendicular to the pressure axis. Therefore the measurement corresponds to the thermal diffusivity perpendicular to the fiber axis. Due to the low transverse TC of the fiber (5 $W\,m^{-1}\,K^{-1}$), it should be noted that we measured the lowest thermal diffusivity of our composite material. Measures were

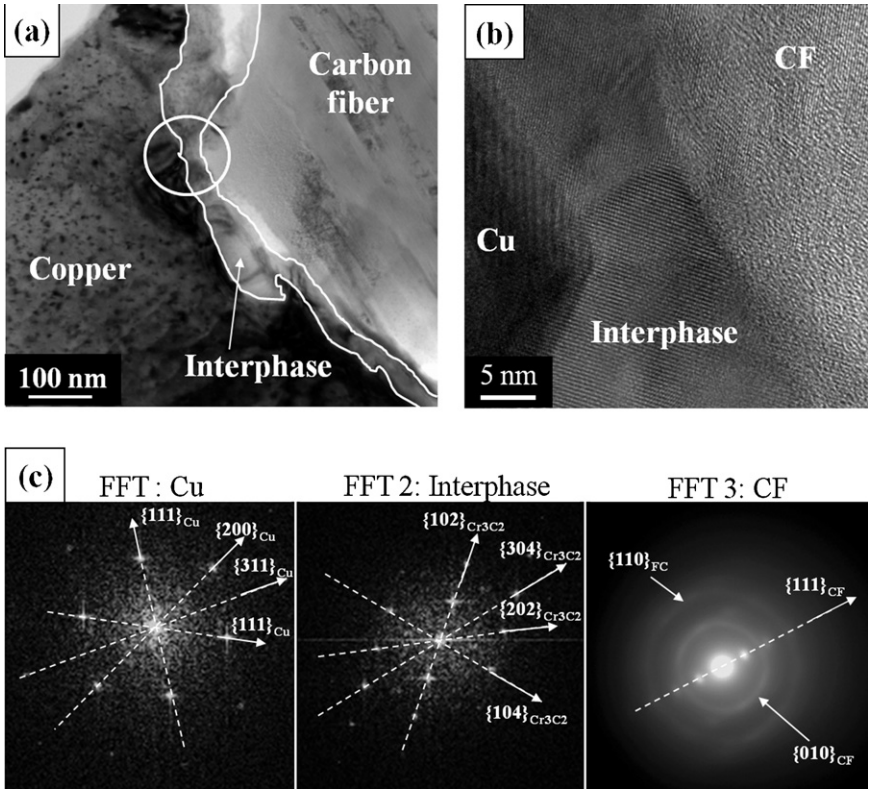

Fig. 7. TEM micrographs (a) of the Cu–Cr/CF composite material after annealing treatment, (b) magnification of the circled area in (a) and (c) diffraction pattern inside the copper, the interphase and the CF.

taken for both Cu–Cr/CF and Cu–B/CF composites. The calculated TC from the experimental thermal diffusivities are given in Table 2.

The first point that could be highlighted is the higher TC of the composite materials with the XN100 CF compared to those with the CN80C fibers. However, it should be noticed that both CF have the same TC in transverse direction but a different one along the CF axis (Table 1). The difference of TC measured between these two sets of composite materials could only be explained by an imperfect orientation of the CF inside the matrix. Indeed, if the CF are not perfectly perpendicular to the pressure direction, a parallel contribution on the TC must be taken into account. This phenomenon has already been demonstrated [12] in the case of a Cu/carbon nanofibers (CNF) composite material using finite element simulation. The calculated TC perpendicular to the CNF axis increases with the orientation of the CNF, as shown in Fig. 8.

Another observation is the similar TC values of composites with same reinforcement and different matrices (Cu or Cu–Cr or Cu–B), while the initial TC of the pure matrices are different. Indeed, the copper alloy matrices (Cu–Cr and Cu–B) have a lower TC than pure Cu whereas the final composites have the same TC. This phenomenon can be explained by the diffusion of the alloying

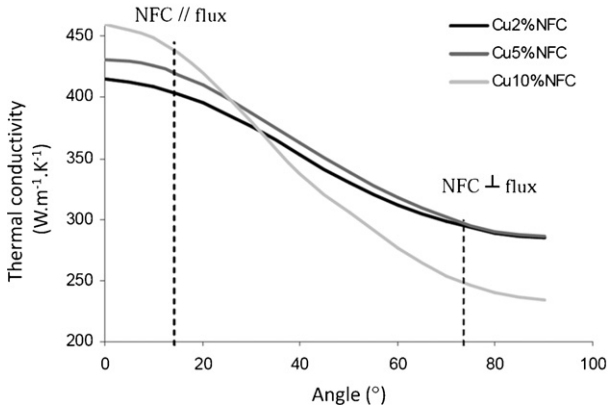

Fig. 8. Variation of the thermal conductivity with the orientation of the reinforcement in a Cu/CNF composite material [1].

Table 2
Transverse thermal conductivity and parallel CTE of Cu–X/CF composite materials.

Matrix	Reinforcement	Sample name	Thermal conductivity ($W m^{-1} K^{-1}$)	CTE ($10^{-6} K^{-1}$)
Cu	–	S1	400	17
	30 vol.% CN80C	S2	180	14
	30 vol.% XN100	S3	220	14
Cu–Cr	–	S4	360	17
	30 vol.% CN80C	S5	180	12
	30 vol.% XN100	S6	190	14
Cu–B	–	S7	370	17
	30 vol.% CN80C	S8	180	12
	30 vol.% XN100	S9	230	13

element at the Cu/CF interfaces which leads to the formation of a carbide at the interface and a matrix almost free of alloying element. This means that the value of the TC depends mostly on the TC of the matrix and reinforcement and not on the interface type (mechanical or chemical).

3.4.2. Coefficient of thermal expansion (CTE)

As mentioned previously, the densification process leads to a random orientation of the CF in a plane perpendicular to the pressure direction. Table 2 shows the CTE variation, inside this plane, for different Cu/CF and Cu–X/CF composites.

3.4.2.1. Several points should be emphasized.

- Whatever the matrix used (pure Cu or Cu alloys), the addition of CF inside the matrix leads to a decrease of the CTE of the composite material.
- For Cu/CF composites, where there is no chemical interface between the matrix and the reinforcement, CTE values are identical for both CF (CN80C and XN100). Therefore the decrease of the CTE is mainly attributed to a composite effect where the mechanical clamping of the CF by the Cu matrix allows a transfer of properties between the matrix and the reinforcement. Indeed, if we assumed that the CF are perfectly oriented in the plane but randomly dispersed, a simple rule of mixture will give an average CTE value of the CF equal to $5.5 \times 10^{-6}\,K^{-1}$ and for the composite close to $14 \times 10^{-6}\,K^{-1}$. Our experimental values are in very good agreement with this simple rule of mixture.
- For Cu–X/CF composites, with Cu–Cr or Cu–B matrices, an improvement of the CTE compared to the Cu/CF reference composite is measured. It should be noted that CTE measured for copper alloy composites with CN80C fibers are slightly lower than those with XN100. Chemical analyses on both CF provide some hypothesis to this small but real effect. XPS analyses on both fibers show a similar behavior where C_{1s} linked to graphite is mainly obtained. However, Raman analyses on both fibers give different results. Raman spectroscopy is used to measure the crystallinity of the fiber. Indeed, if the CF is perfectly crystalline, only one peak close to 1580 cm^{-1}, corresponding to the G-band of graphite, appears in the Raman spectrum. When defects are present in the volume of interrogation, another peak called disorder-induced band (D-band) is detected around 1350 cm^{-1}. The intensity ratio between the G-band and the D-band (I_G/I_D) can be linked to the defect quantity on the CF surface. Raman spectroscopy analyses of CN80C and XN100 fibers give values of I_G/I_D of 4.5 and 7.3, respectively. These ratios confirm the higher quantity of crystalline defects on the CN80C fiber, therefore this type of CF is more reactive if we assume that defects are linked to the nucleation sites for carbide formation. Finally, stronger chemical interfaces are present between copper alloy matrices and CN80C CF than with XN100 CF. These stronger chemical links can be associated to higher transfer properties which result in lower measured CTE.

3.4.2.2. Influence of the annealing treatment. An optimized annealing treatment has been performed (1000 °C, 24 h, under reducing atmosphere) on the composite with the lowest CTE (sample S5, Cu–Cr/CN80C) in order to increase the diffusion of the alloying element (Cr) toward the Cu/CF interface. This diffusion phenomenon is clearly seen in the chemical analyses (Section 3.3) and the formation of chromium carbide is identified. In order to quantify the effect of this chemical interface, the same treatment was performed on a reference sample having only a mechanical interface (sample S2, Cu/CN80C). The CTE of both samples have been measured before and after annealing treatment.

The annealing treatment on the reference sample (sample S2) lead to a deterioration of the thermo-mechanical properties, the CTE value of this sample increasing from $14 \times 10^{-6}\,K^{-1}$ to $17 \times 10^{-6}\,K^{-1}$. As explained previously, there is no chemical reaction between Cu and CF therefore the interfacial link is only a mechanical link due to the CTE mismatch between the Cu and the CF. The annealing treatment was made at 1000 °C without any constraint; therefore the dilatation of Cu was much higher than that of the CF and lead to a delamination between the matrix and the reinforcement, and a destruction of the mechanical interface. Therefore pure copper matrix CTE is measured after this heat treatment.

However, in the case of sample S5 where a chemical interface is present, we observe a decrease of the CTE from $12 \times 10^{-6}\,K^{-1}$ to $11 \times 10^{-6}\,K^{-1}$. The annealing treatment is advantageous in this case because it leads to the full diffusion of the alloying element toward the interfacial zone and the formation of a stronger carbide chemical bond (Cr_3C_2) at the Cu/CF interface. This chromium carbide interphase preserves the contact between the matrix and the reinforcement and avoids delamination of the material which results in a decrease of the composite material CTE.

These thermo-mechanical analyses show that the addition of an alloying element (chromium) produces thermal conductivity equivalent to Cu/CF composites, but with an improvement of 25% for the CTE.

4. Conclusions

The chemical and microstructural characterizations of the Cu–X/CF composite materials have shown diffusion of the alloying element (X = Cr or B) in the copper matrix toward the copper/carbon fiber interface. Analyses at a nanometric scale have clearly identified the crystalline structure of the interfacial zone, *i.e.* chromium carbide (Cr_3C_2) for the Cu–Cr/CF composites and boron carbide (B_4C) for the Cu–B/CF. Measurements of thermo-mechanical properties for each composite has demonstrated the influence of the interfacial zone composition and the reinforcement type on the material properties. We have produced a promising composite by adding chromium in the copper matrix and using CN80C carbon fibers as reinforcement. Compared to a similar composite material without alloying element, an improvement of 25% on the coefficient of thermal expansion was measured.

Acknowledgement

The authors would like to thank the "Programme inter-région Midi-Pyrénées/Aquitaine, Cuivre allié/nanofibre de carbone" for its financial support.

References

[1] A. Luedtke, Adv. Eng. Mater. 6 (3) (2004) 142–144.
[2] C. Zweben, JOM 50 (6) (1998) 47–51.
[3] P.-M. Geffroy, et al. Mater. Sci. Forum 534–536 (2007) 1505–1508.
[4] J.-D. Mathias, et al. Appl. Therm. Eng. 29 (11–12) (2009) 2391–2395.
[5] T. Schubert, et al. Scripta Mater. 58 (4) (2008) 263–266.
[6] L. Weber, et al. Scripta Mater. 57 (11) (2007) 988–991.
[7] K. Chu, et al. J. Alloys Compd. 490 (1–2) (2010) 453–458.
[8] J.-F. Silvain, et al. J. Mater. Chem. 10 (9) (2000) 2213–2218.
[9] A. Veillère, et al. Acta Mater. (2010), doi:10.1016/j.actamat.2010.11.006.
[10] A. Veillère, Drains thermiques adaptatifs: Cuivre allié/Fibre de Carbone, Ph.D. Thesis, Université Sciences et Technologies – Bordeaux I, 2009.
[11] K.D. Childs, et al., Handbook of Auger Electron Spectroscopy, Phys. Elec. Inc., 1995
[12] C. Vincent, Le composite cuivre/nanofibres de carbone, Ph.D. Thesis, Université Sciences et Technologies – Bordeaux I, 2008.
[13] J.P. Gwinn, et al. Microelectron. J. 34 (2003) 215–222.